

Article

# Stability Study of Erythritol as Phase Change Material for Medium Temperature Thermal Applications

Mayra Paulina Alferez Luna , Hannah Neumann and Stefan GschwanderFraunhofer Institute for Solar Energy Systems, Heidenhofstr. 2, 79110 Freiburg, Germany;  
hannah.neumann@ise.fraunhofer.de (H.N.); Stefan.gschwander@ise.fraunhofer.de (S.G.)

\* Correspondence: mayra.alferez.luna@ise.fraunhofer.de; Tel.: +49-(761)-4588-2016; Fax: +49-761-4588-9000

**Abstract:** Sugar alcohols belong to a promising category of organic phase change materials (PCM) because of their high latent heat and density compared to other PCM. However, some sugar alcohols have shown latent heat degradation when heated above their melting temperature. Most of the available studies report the structural changes of erythritol during cycling rather than its thermal stability at constant temperature. This study aimed to assess the effect of thermal treatment on erythritol thermal, chemical and physical properties, as well as to find means to enhance its thermal stability. Erythritol and its mixtures with antioxidant were heated and maintained at different temperatures above its melting point. Erythritol was analyzed before and after thermal treatment via Fourier-transform infrared spectroscopy and differential scanning calorimetry. It was suggested that the degradation of latent heat follows a first order reaction. Mixtures of erythritol with antioxidant had a lower degradation rate compared to pure erythritol under air. Sample browning was observed along the heating treatment of mainly pure erythritol. Antioxidant was found to help to reduce erythritol degradation. No chemical composition changes were detected in samples under argon atmosphere and overall good thermal stability was found throughout the testing period.



**Citation:** Alferez Luna, M.P.; Neumann, H.; Gschwander, S. Stability Study of Erythritol as Phase Change Material for Medium Temperature Thermal Applications. *Appl. Sci.* **2021**, *11*, 5448. <https://doi.org/10.3390/app11125448>

Academic Editor: Ioannis Kartsonakis

Received: 10 May 2021

Accepted: 9 June 2021

Published: 11 June 2021

**Publisher's Note:** MDPI stays neutral with regard to jurisdictional claims in published maps and institutional affiliations.



**Copyright:** © 2021 by the authors. Licensee MDPI, Basel, Switzerland. This article is an open access article distributed under the terms and conditions of the Creative Commons Attribution (CC BY) license (<https://creativecommons.org/licenses/by/4.0/>).

**Keywords:** phase change material; sugar alcohol; erythritol; latent heat storage; thermal stability; degradation kinetics

## 1. Introduction

An efficient use of renewable energy resources, such as solar energy, is increasingly being considered as a promising solution to global warming. However, solar energy is intermittent in nature and its intensity depends on the hour of the day and local weather conditions [1,2].

It is necessary to establish thermal energy storage (TES) technologies in order to steadily utilize the unused thermal energy. The main role of energy storage systems is to reduce the time or rate mismatch between energy supply and energy demand [3]. In Europe, it has been estimated that around 1.4 million GWh per year can be saved and 400 million tons of CO<sub>2</sub> emissions avoided in buildings and in industrial sectors by more extensive use of heat and cold storage [4].

Sensible and latent heat storage are considered as the basic types of TES techniques. Sensible heat storage (SHS) is based on the temperature change in the material. SHS systems use the heat capacity and the change in temperature of the storage medium during the charging/discharging process. Therefore, the temperature of the storage material increases when energy is absorbed and decreases when energy is released [5]. Latent heat storage (LHS) is based on the heat absorption and release when the storage medium undergoes a phase change. A solid-liquid phase change via melting and solidification can store large amounts of thermal energy. Usually, a small volume change ( $\leq 10\%$ ) occurs upon melting. Therefore, the pressure is not changed significantly and, hence, melting and solidification of the storage material proceed at a constant temperature. Upon melting, the

storage material keeps its temperature constant at the melting temperature, which is also called temperature of transition [6]. Stored latent heat during the phase change process is calculated from the enthalpy difference ( $\Delta H$ ) between the solid and liquid phase, which is called melting enthalpy or heat of fusion.

Phase change material (PCM) can be used to store thermal energy or to control the temperature swings within a specific temperature range. The operating principle of PCM is the following: as the temperature rises and reaches its melting temperature, PCM absorbs heat in an endothermic process and changes phase from solid to liquid. Similarly, as the temperature drops under its melting temperature, PCM releases heat in an exothermic process and returns to its solid phase [7]. According to its properties, PCMs have several application possibilities. A PCM filled window system was proposed by Ismail and Henriquez [8] taking advantage of the translucent and thermal properties of the selected PCM. Some PCMs are highly transparent for the visible part of solar radiation whereas the infrared part is absorbed within the PCM, which allows both the advantages of a daylighting element and of energy storage to be achieved [9]. In addition, coconut fat recovered from underused feedstocks have been used as bio-based PCM for its application in building envelopes due to its good physical, chemical and thermal properties [10].

Sugar alcohols (SA), also called polyols [11], are attractive bio-based materials to be used as PCM. Additionally, as by-products from the food industry, SA are non-corrosive, non-toxic and environmentally friendly [12]. They have great potential in many TES applications due to their high mass and volume-specific melting enthalpies compared to other organic PCM [13]. SA have melting temperatures ranging between 90 and 200 °C. However, some SA are not stable at higher temperatures [6].

Erythritol is a promising organic PCM for recovering solar energy and industrial waste heat at temperatures up to 160 °C [14]. Erythritol is a material emerging as PCM due to its attractive TES properties. Erythritol's melting point varies in literature [11,14–16] between 117 °C and 119 °C according to its purity percent and manufacturer. In addition, it has a high latent heat of 340 J/g, almost equivalent to that of the ice to liquid water phase change.

Kaizawa et al. [14] studied the thermophysical properties of erythritol using differential scanning calorimetry (DSC), thermogravimetry-differential thermal analysis (TG-DTA) and a heat storage tube. Palomo del Barrio et al. [11] carried out an experimental characterization of erythritol by measuring their physical properties such as specific heat and thermal conductivity, among others. The suitability of erythritol as PCM was examined by Kakiuchi et al. [15] according to its thermodynamic, kinetic and chemical properties. Zhang et al. [17] found that the crystal growth speed of some SA is highly dependent on temperature, whereas Lopes Jesus et al. [18] claimed that the solid erythritol obtained from the melt has different degrees of crystallization depending on the used cooling rate. Some eutectic mixtures have also been studied, such as erythritol-xylitol or erythritol-sorbitol [19], and erythritol-based composites with the addition of expanded graphite and carbon nanotubes were also evaluated by Guo et al. [20]. However, all these studies addressed thermal cycling tests rather than erythritol thermal stability at constant temperature, which would allow a degradation rate to be determined under conditions closer to real operation. On the other hand, Nomura et al. [16] investigated the heat release performance of a direct-contact heat exchanger using erythritol as PCM along with a heat-transfer oil. The suitability and appropriate parameters for charging and discharging erythritol to power a LiBr/H<sub>2</sub>O absorption cooling system were assessed by Agyenim et al. [21]. Kaizawa et al. [22] studied the thermal and flow behaviors in a trans-heat container filled with erythritol as part of a waste heat transportation system. Nevertheless, the conclusions made by these authors are ambiguous about the performance of erythritol as PCM.

Therefore, this study aims to investigate the effect of thermal treatment on the erythritol thermal properties at constant temperatures above its melting point. The experiments are also conducted under an inert atmosphere and an antioxidant is added to the samples. Degradation rates at different temperatures and conditions (under air/inert atmosphere

and with/without antioxidant) are calculated. In addition, degradation kinetics with respect to its latent heat are evaluated. A mechanism of oxidation of erythritol under air is proposed, as well as the possible underlying mechanism on the stability enhancement of erythritol by antioxidant. The reaction pathway of thermal dehydration of erythritol and the likely relationship between dehydration and oxidation products with the sample browning are suggested

## 2. Materials and Methods

### 2.1. Materials

Zerose™ Erythritol with a purity of 99.5% was purchased from Cargill and used without further treatment. Irganox 1010® from BASF [23] was used as antioxidant. Irganox 1010® is a phenolic antioxidant which has been used to stabilize organic polymers against thermal oxidative degradation [24,25].

### 2.2. Sample Preparation

Samples were prepared in a mortar by manually grinding and mixing erythritol with 5 wt.% of antioxidant. An amount of  $220 \pm 0.4$  mg of each sample was filled into the glass vials (1.5 mL, ND11) and then sealed using a PTFE/silicon septum and an aluminum crimp cap. In order to create an anoxic environment inside the vials, some samples were purged with argon for 10 min by using two cannulas as inlet and outlet. Samples that did not get further treatment after the sealing process were used to assess the degradation under air atmosphere. Pure erythritol samples were also used as blanks for each experiment. All samples were weighed after sealing them using a Secura® Analytical Balance from Sartorius (224-1S) with an uncertainty of  $\pm 0.1$  mg.

The glass vials filled with the samples were placed in aluminum blocks according to their atmosphere (air and argon). Each of these blocks had an aluminum lid, which was attached with four screws (Figure 1). For the experiments under argon atmosphere, a gas inlet and outlet of the aluminum blocks was connected with a plastic hose to nitrogen stream, which flowed through the block continuously (Figure 1). A continuous flow rate of  $30 \text{ cm}^3/\text{min}$  of nitrogen was used then to reduce the traces of oxygen that may have remained between the block cavities and the glass vials, as well as to prevent it from entering the vials.

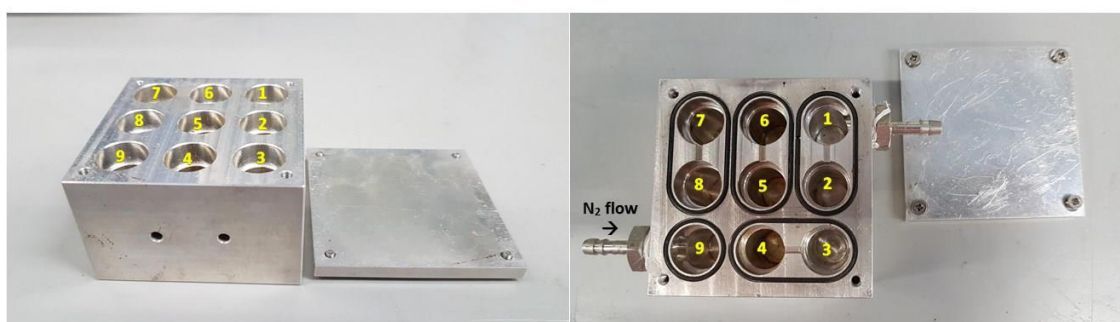


**Figure 1.** Left: aluminum block used for tests under air. Right: aluminum block with gas inlet and outlet for tests under argon atmosphere.

### 2.3. Thermal Treatment

Once the aluminum blocks were loaded with the sample vials, they were heated and maintained at a constant temperature of  $121 \text{ }^\circ\text{C}$ ,  $131 \text{ }^\circ\text{C}$  and  $141 \text{ }^\circ\text{C} \pm 1 \text{ }^\circ\text{C}$ , respectively. After  $10 \pm 5$  h, one vial after the other was taken out of the aluminum block. Samples of pure erythritol under air and under argon with antioxidant at  $141 \text{ }^\circ\text{C}$  had a shorter heating time ( $8 \pm 4$  h) due to the technical capacity in the lab. This method allowed all batch samples (9 samples per block) to be exposed to the heating temperature for different periods of time, and hence, changes in the melting enthalpy could be assessed while

increasing the thermal treatment time. Thermal degradation tests were performed for about a maximum of 100 h. In addition, samples of pure erythritol under argon atmosphere and with 5 wt.% antioxidant under air, both at 141 °C, were assessed over a period of 935 h. Table 1 summarizes the performed experiments.

**Table 1.** Summary of the performed experiments.

Atmosphere	Sample	Temperature [°C]	Thermal Treatment Time	Test Duration
Air	Erythritol	121	100 h	Short-term-test
	Erythritol/Antiox		100 h	Short-term-test
	Erythritol	131	100 h	Short-term-test
	Erythritol/Antiox		100 h	Short-term-test
	Erythritol	141	78 h	Short-term-test
	Erythritol/Antiox		100 h	Short-term-test
Argon	Erythritol	121	100 h	Short-term-test
	Erythritol/Antiox		100 h	Short-term-test
	Erythritol	131	100 h	Short-term-test
	Erythritol/Antiox		100 h	Short-term-test
	Erythritol	141	100 h	Short-term-test
	Erythritol/Antiox		74 h	Short-term-test
Air	Erythritol/Antiox	141	935 h	Long-term-test
Argon	Erythritol		935 h	Long-term-test

After the samples cooled down to room temperature, they were weighed again. An inert atmosphere was also kept for the samples prepared under argon until they solidified. Finally, each sample was taken out from its vial and processed into a homogeneous mix via manual grinding in a mortar. It is important to note that all samples were already solid when ground to avoid further effects in the melting enthalpy. Keeping an inert atmosphere while the samples were melted was relevant in order to assess if such atmosphere affects the melting enthalpy during the heating.

#### 2.4. Differential Scanning Calorimetry (DSC) Characterization

Latent heat of fusion of the samples after the thermal treatment described in Table 1 was determined via differential scanning calorimetry using a Discovery DSC 2500 manufactured by TA Instruments with an uncertainty of 2%. The DSC cell was purged with 50 mL/min nitrogen while measuring the sample. After the heating procedure described in Section 2.3, sample amounts of about 8–9 mg were placed in Tzero<sup>®</sup> aluminum pans with aluminum pierced lids. An inert atmosphere was maintained during the whole cycling. Each sample was analyzed in triplicate and the obtained data were averaged. The DSC tests comprised three different cycles. During the first cycle, the sample was heated to 130 °C and then cooled down to 0 °C, both with a heating rate of 10 K/min. Isothermal periods of five minutes were added after reaching both temperature limits (0 °C and 130 °C). The next two cycles were carried out at a heating rate of 1 K/min following the same process of the first cycle. The data were collected from the last heating cycle. Obtained data were analyzed using TRIOS v4.1.1.33073 software.

#### 2.5. Proposed Kinetic Model of Latent Heat Degradation

Thermal degradation of tests performed at different temperatures was evaluated using constant temperature kinetics based on latent heat (L) measured via DSC according to Sagara et al. [26]. A fraction of reaction ( $\alpha$ ) was defined according to Equation (1) as the

change with respect to the initial material property. Thus,  $L_t$  is the recorded latent heat after the heat treatment at a certain time,  $t$ , while  $L_0$  is the latent heat before the heat treatment.

$$\alpha = 1 - \frac{L_t}{L_0} \quad (1)$$

Kinetics of thermal degradation is usually based on Equation (2):

$$\frac{d\alpha}{dt} = K \cdot f(\alpha) \quad (2)$$

where  $\alpha$  is the fraction reacted in time  $t$ , and  $f(\alpha)$  is the reaction model, which depends on the reaction mechanism according to different physical models [27–29]. Finally, the rate constants ( $k$ ) for each test were calculated at three different temperatures (121 °C, 131 °C and 141 °C), and the Arrhenius parameters were determined according to Equation (3):

$$K = A \cdot e^{\frac{-E_a}{RT}} \quad (3)$$

## 2.6. Fourier-Transform Infrared Spectroscopy (FTIR) Analysis

Erythritol thermal stability and changes in its molecular scale, bonds and functional groups after being heated at three different constant temperatures (121 °C, 131 °C and 141 °C) were assessed with a Fourier transformation infrared spectrum analysis (FTIR). FTIR measurements were carried out before and after the thermal treatment in the heating chamber described in Section 2.3. FTIR spectra were recorded on a Spectrum Two™ FT-IR spectrometer from PerkinElmer, in the region 4000–450  $\text{cm}^{-1}$ . The obtained data were analyzed with PerkinElmer Spectrum™ 10 software and OriginPro 9.1.

## 3. Results and Discussion

### 3.1. Mass Loss

The measured time-dependent mass loss percentages were fitted in a linear regression based on the least squares method. Mass loss rates were represented as the slope of the linear regression, while the uncertainty of each rate was described as the standard error of the given slope. Figure 2a shows the results of all tests.

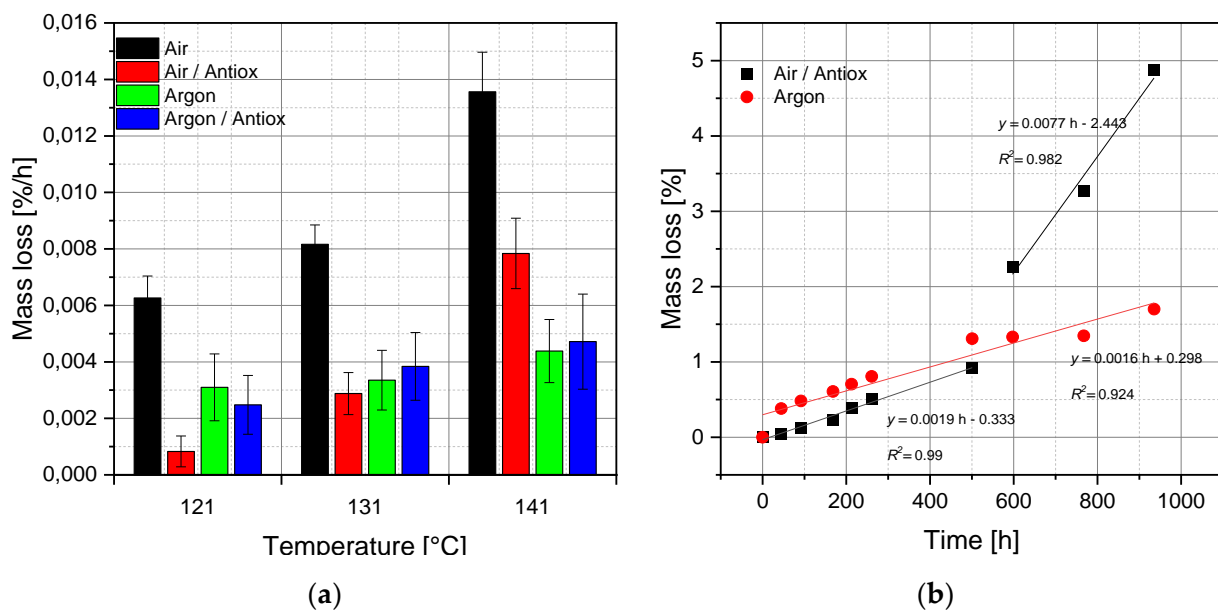


**Figure 2.** (a) Percentage of mass loss per hour at 121 °C, 131 °C and 141 °C for short-term tests. (b) Percentage of mass loss at 141 °C for long-term test.

Samples of pure erythritol under air registered the highest mass loss rates along the short-term heating treatment:  $0.0063 \pm 0.0008\%/h$ ,  $0.0082 \pm 0.0007\%/h$  and  $0.0136 \pm 0.0014\%/h$  at 121 °C, 131 °C and 141 °C, respectively. An upward trend in the percentage of mass decrease regarding heating temperature for both groups of short-term tests under air was registered. The use of antioxidant helped to diminish the temperature effect on the mass content loss of samples under air as seen in Figure 2a. When heated at 141 °C and after 935 h (long-term test) erythritol with antioxidant under air lost nearly 5% of its mass. However, it seems that the antioxidant was consumed during the first 600 h, since after 597 h its mass loss rate tripled the initial one, as shown in Figure 2b.

Regarding samples under argon atmosphere, a mass loss rate increase was also recorded. Temperature, however, had a lighter impact on these results in comparison with the registered values of the samples under air. In addition, adding antioxidant did not have a major impact on the samples under Argon. Vials were weighed before and after filling them with argon, as well as after the heating procedure. As a result of the argon purge, vials were not completely sealed anymore due to the use of cannulas on the lids. Thus, by the end of the experiment it was not possible to assure that the registered mass loss was related only to the sample itself and not to a loss of argon during the heating treatment.

Erythritol mass loss could be associated to oxidation and dehydration reactions. During oxidation, several fragmentation products can be formed (see Section 3.4). Fragmentation produces low molecular weight products with high vapor pressures. Fragmentation products may then evaporate, increasing the mass loss rate. In addition, dehydration of erythritol yields 1,4-erythritane, which can be further dehydrated to form carbonyl compounds also affecting the mass loss ratio. Samples of pure erythritol were more susceptible to oxidization due to the higher oxygen availability in comparison to samples with antioxidants or argon. Dehydration reactions may also have followed. Therefore, mass loss rates of pure erythritol at the three tested temperatures were also the highest. On the other hand, mass loss of both types of samples under argon is more likely related to dehydration reactions of erythritol. Kakiuchi et al. [15] claimed that the degradation of erythritol depends on oxygen concentration. In addition, as it is known, increasing the temperature at which a reaction takes place generally speeds up the rate of reaction. These last two statements can also be confirmed in Figure 2a.

### 3.2. Latent Heat Degradation

As described in Section 2.4, each sample was analyzed in triplicate and the obtained data were averaged. The standard deviation of each sample was estimated from the calculated average and presented as error bars.

Figure 3a depicts the results of the latent heat degradation for the short-term experiments at 141 °C. Pure erythritol under air suffered the highest latent heat loss over time. A latent heat reduction of 22.7% regarding the initial value was registered. Adding antioxidant helped to improve the thermal stability of samples under air. However, due to the fact that enthalpy is an extensive property, its magnitude is proportional to the amount of the substance that reacts. Therefore, the latent heat value is reduced by the percentage of added antioxidant. The enthalpy of fusion of samples with antioxidant will then be lower than the value of the polyol itself, as it is also shown in Figure 3a. Both experiments under argon atmosphere registered lower latent heat reductions in comparison with erythritol under air. Pure erythritol and erythritol-antioxidant lost 2.8% and 2% of their initial enthalpy values by the end of the test, respectively.

Registered latent heat values were fitted in a linear regression in order to get the degradation rates for all experiments (Figure 3b). An upward trend in the latent heat degradation rate regarding heating temperature was registered for all experiments, with the highest degradation rates for pure erythritol under air. Samples with antioxidant under air showed lower latent heat degradation rates than pure erythritol samples. Latent heat degradation rates of  $0.13 \pm 0.030$  kJ/(kg h),  $0.14 \pm 0.024$  kJ/(kg h) and  $0.15 \pm 0.021$  kJ/(kg h) were registered for samples at 121 °C, 131 °C and 141 °C with antioxidant under air,

respectively. This represents about 3 to 4 times less than samples without any additive and under air. Thus, it seems that the temperature rise in combination with antioxidant did not influence the degradation rates of samples under air as much as those of the samples of pure erythritol under air. However, the degradation rate during the long-term test starts to increase from 260 h onwards to a value of  $0.19 \pm 0.005$  kJ/(kg h), which could be due to the gradual consumption of antioxidant during the experiment of 935 h (Figure 4a).

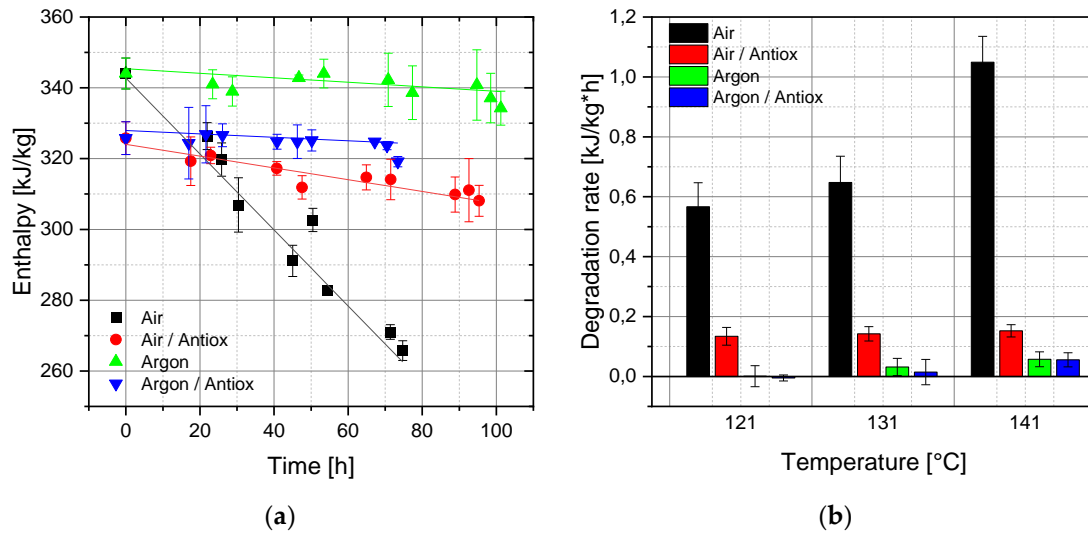


**Figure 3.** (a) Evolution of latent heat values over time during the short-term experiment at 141 °C. (b) Latent heat degradation rate for short-term tests at three different temperatures.

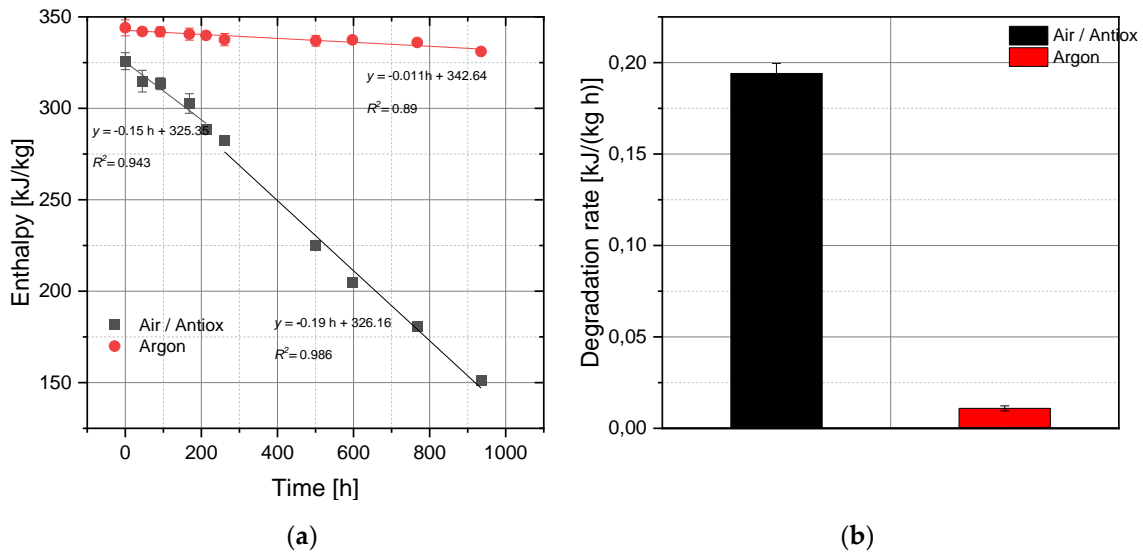


**Figure 4.** (a) Evolution of latent heat values over time during long-term experiments at 141 °C. (b) Latent heat degradation rate for long-term experiments at 141 °C.

Likewise, Figure 3b shows that lower degradation rates were obtained for both experiments conducted under argon atmosphere, the highest one being  $0.06 \pm 0.02$  kJ/(kg h) for tests at 141 °C. Since the latent heat of fusion recorded from tests under an argon atmosphere decreased less than under air, the slopes of linear fittings were close to zero, resulting in a high standard deviation of the slope. In addition, Figure 4a depicts how the latent heat of fusion of the samples under an argon atmosphere decreased less by the end of the long-term test than those with antioxidant under air, with an average degradation

rate of only  $0.01 \pm 0.001$  kJ/(kg h), as shown in Figure 4b. This indicates that an anoxic environment diminishes the erythritol degradation for exposure times up to 935 h.

Latent heat decrease of sugar alcohols after heating has previously been reported [30,31]. It is suggested that the hydrogen bonding structure of erythritol can be weakened and eventually destroyed by temperature increasing, which in turn may cause a decrease in its latent heat [32,33]. Inagaki and Ishida [34] claimed that in the case of sugar alcohols a majority of the released/stored thermal energy originates from the change of electrostatic interaction energy associated with formation/disruption of intermolecular hydrogen bonds in the solid–liquid phase transition. That is, a larger number of intermolecular hydrogen bonds in the solid phase causes a stable solid phase in terms of electrostatic energy. In addition, Matuszek et al. [35] found that latent heat depends on the concentration and strength of hydrogen bonding present in the crystal structure and on the extent of disruption of the crystal phase at elevated temperatures. The same author mentioned that an ideal PCM is one in which many strong hydrogen bonds are present in the crystalline phase and which are readily disrupted on melting. A decrease in latent heat may also be attributed to incomplete crystallization during cooling from the melt. In the case of erythritol, it did not crystallize completely while increasing the temperature of the heating treatment (see Section 3.4). Thus, less energy was required to melt the sample than it would have needed if it had crystallized entirely.

### 3.3. Kinetic Analysis of Latent Heat Degradation

Kinetics of thermal degradation is usually based on Equation (2). After rearrangement and integration, Equation (2) becomes Equation (4)

$$\int_0^\alpha \frac{d\alpha}{f(\alpha)} = k \int_0^t dt \quad (4)$$

where the left side of the equation is the integrated form of the reaction model  $g(\alpha)$ , according to Equation (5)

$$\int_0^\alpha \frac{d\alpha}{f(\alpha)} = g(\alpha) \quad (5)$$

Substitution of Equation (5) in Equation (4) leads to Equation (6)

$$g(\alpha) = k \cdot t \quad (6)$$

where  $g(\alpha)$  is the integrated reaction model. Selecting the best-fit reaction model in Equation (6) gives a straight line by plotting  $g(\alpha)$  versus time  $t$ . Nomura et al. [36] showed that a first order reaction, expressed as  $-\ln(1 - \alpha)$ , is suitable to describe the degradation of the latent heat of sugar alcohols.

As could be seen in Section 3.2, melting enthalpy values obtained from tests under an argon atmosphere remained more stable over time. The 100 h test period was rather short to observe significant latent heat changes. Therefore, the reaction kinetics for tests under an argon atmosphere were not assessed. Figures 5a and 6a depict the data obtained for tests of pure erythritol under air and with antioxidant at the three given temperatures, respectively.

The rate constant ( $k$ ) was determined from the slope of the straight line. Furthermore, the rate constants ( $k$ ) were calculated at the three given temperatures and the Arrhenius parameters were determined according to Equation (3). Figures 5b and 6b show the Arrhenius plot for tests of pure erythritol under air and erythritol with antioxidant, respectively.

Reaction rates ( $k$ ) obtained for erythritol under air increased when the temperature increased. These changes were more evident in samples of pure erythritol. Temperature is a factor that affects reaction rates, i.e., an increase in temperature normally increases the rate of reaction. The temperature dependency of reactions is in turn determined by the activation energy. Activation energy ( $E_a$ ) values of 41.65 kJ/mol and 5.55 kJ/mol were calculated according to Equation (3) for tests of pure erythritol under air and erythritol with antioxidant, respectively.

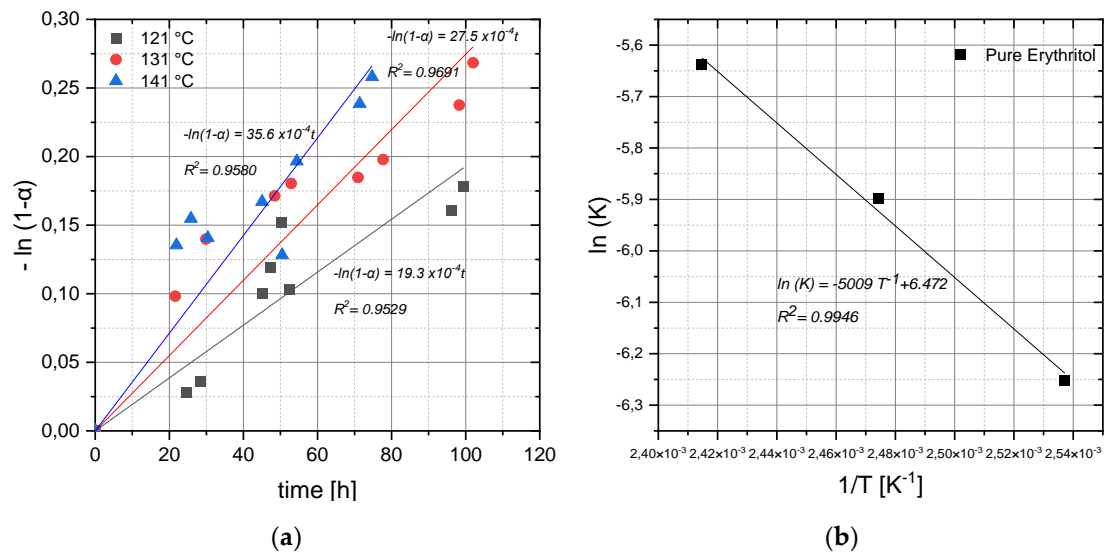


**Figure 5.** (a) Plot of degradation of latent heat  $-\ln(1 - \alpha)$  versus time  $t$  for pure erythritol under air at three different temperatures. Data points were subjected to a least squares fitting. (b) Arrhenius plot for latent heat thermal degradation of pure erythritol under air. Data points were subjected to a least squares fitting.

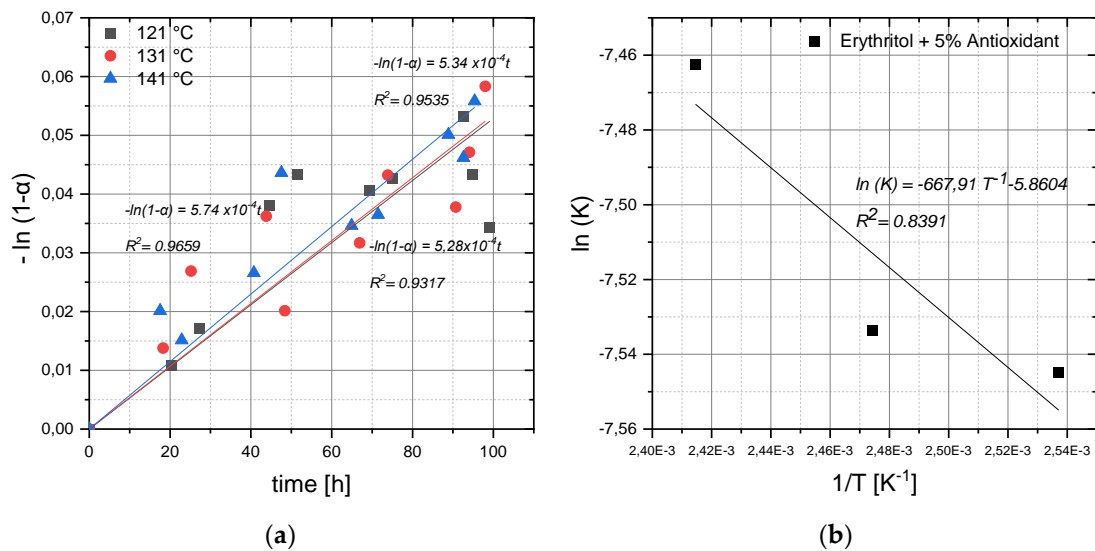


**Figure 6.** (a) Plot of degradation of latent heat  $-\ln(1 - \alpha)$  versus time  $t$  for erythritol with antioxidant under air at three different temperatures. Data points were subjected to a least squares fitting. (b) Arrhenius plot for latent heat thermal degradation of erythritol with antioxidant under air. Data points were subjected to a least squares fitting.

Even though the reaction rates ( $k$ ) of erythritol with antioxidant tend to increase with increasing temperature as shown in Figure 6a, the effect is not as considerable as it is in pure erythritol samples. Antioxidant was found to diminish the thermal degradation during heating under air and its corresponding samples were less temperature sensitive than those without any added additive. Temperature-sensitive reactions have high activation energies, that is, the higher the activation energy, the faster the reaction is by increasing temperature.

### 3.4. Chemical Degradation

Samples of pure erythritol under air suffered the most evident physical changes after the thermal treatment. Pure erythritol experienced a significant consistency change, from a loose white powder to a brown sticky paste by the end of the tests. Several samples of pure erythritol under air did not directly solidify after being placed at room temperature.

Erythritol under air became brown with increasing temperature and time under thermal treatment, as can be seen in Figure 7.

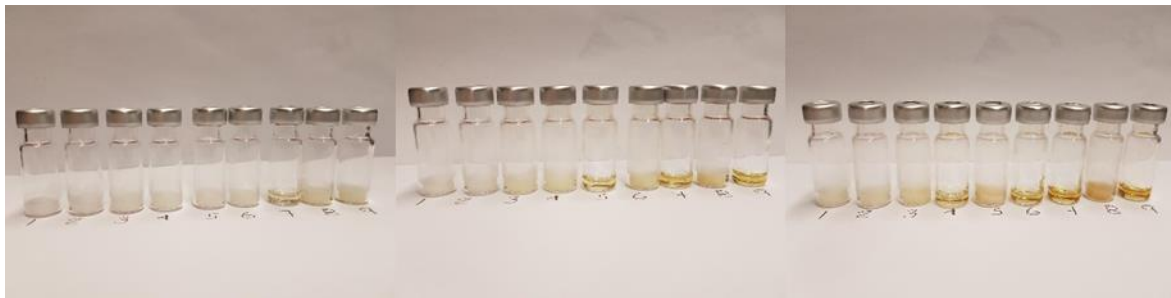


**Figure 7.** Samples of pure erythritol under air for short term at (from left to right) 121 °C, 131 °C and 141 °C.

No exothermic peak was observed in the cooling scan of the sample heated at 141 °C for 78 h, which also did not solidify at room temperature (Figure 8a). This indicates that erythritol became a glass and not a crystal during cooling. The occurrence of a glass transition can be confirmed in the heating scan of the same sample (Figure 8b), in which an exothermic peak can be seen around 6 °C. The latter agrees with the results obtained by other authors [18,37,38]. This exothermic peak corresponds to the cold crystallization of the amorphous phase created in the previous cooling (crystalline phase A). As erythritol was further heated up, a solid/solid transformation took place at around 74 °C, depicted by another small exothermic peak. During solid/solid transformation another crystalline phase similar to the single crystal of meso-erythritol is formed (crystalline phase B) [38]. Afterward, the final crystalline structure melts at around 120 °C. A solid/solid transformation could take place at three different temperature ranges: about 65 °C, between 15 and 43 °C and about 75 °C. All heating curves of Figure 8b show exothermic peaks around the aforementioned temperature ranges. Each type of solid/solid transformation that takes place is related to the different paths of the erythritol's crystallization process. The solid/solid transformation has been reported as an entropically driven process, since heat is not involved [18,37]. However, the exothermic peaks that appeared in the heating scans suggest that the solid/solid transformation that occurred involved heat. Similar results were obtained by Nakano et al. [38]. In addition, melting peaks shifted to lower temperatures while increasing the heating treatment time of the sample. Other sugar alcohols have showed similar melting temperature shifting as treatment time or temperature was increased [31,37]. The presence of four hydroxyl groups in erythritol gives rise to a system of intermolecular and intramolecular hydrogen bonds. Molecular structure and properties, such as melting point, are related to hydrogen bonding [33]. The length and strength of hydrogen bonds are sensitive to temperature, as both vary with temperature quadratically [39]. Thus, the melting point could be reduced by weakening the hydrogen bonding when heating the material.

Erythritol with antioxidant under air suffered a slight browning compared with the samples without additive. Samples that were kept longer in the heating chamber suffered the most noticeable changes. On the other hand, pure erythritol under argon barely changed its color along the heating treatment, however, one sample at the highest temperature did not solidify immediately. Sample browning was also not observed in erythritol-antioxidant under argon and all samples solidified at room temperature. Unlike pure erythritol, all erythritol-antioxidant samples under air solidified at room temperature. Burgoa et al. [40] reported that Irganox 1098, a hindered phenolic antioxidant, acted as a nucleating agent in a thermoplastic vulcanizate blend. Zhang et al. [41] claimed that in hindered phenols with a symmetrical structure the formation of hydrogen bonds is high, which leads to agglomeration and crystallization of the system where it is used. Since Irganox 1010 has a high symmetric molecular structure, it may have promoted the crystallization of erythritol. However, further investigation to confirm this latter point is advised.

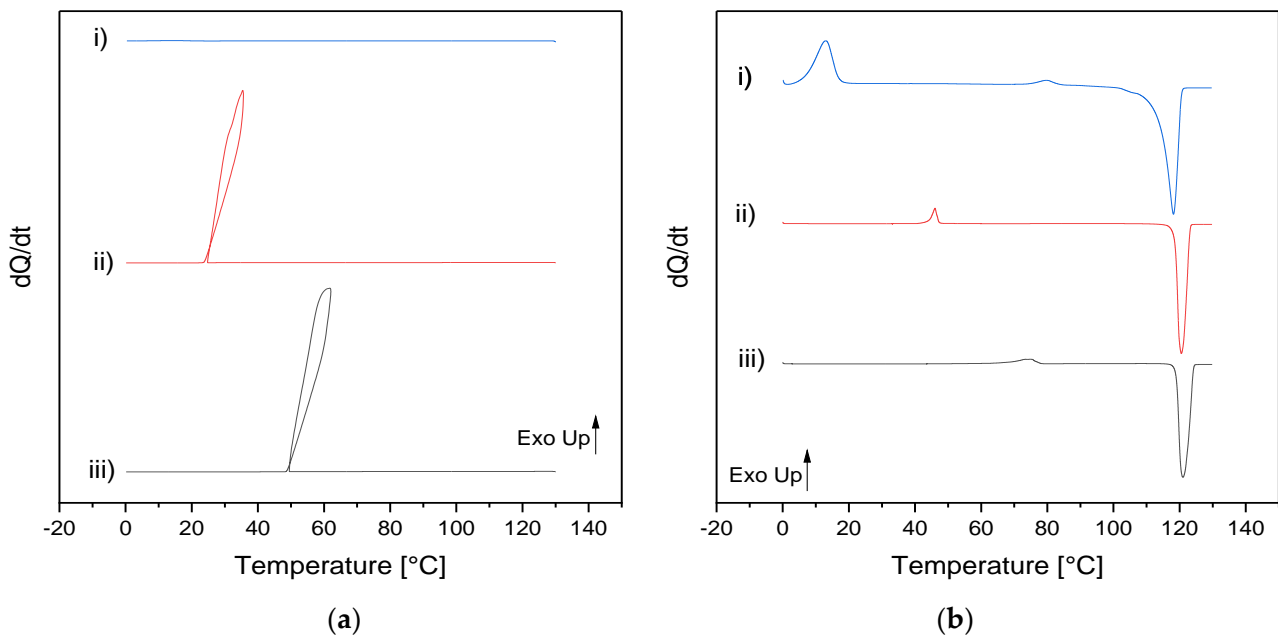


**Figure 8.** DSC (a) cooling and (b) heating scans of pure erythritol samples as received (iii), after 50 h (ii) and after 78 h (i) at 141 °C.

It is assumed that erythritol may undergo oxidation and dehydration reactions. In the presence of air and according to the proposed mechanism of oxidation of erythritol based in reactions already reported in the literature [42–45], hydrogen abstraction either from the carbon chain (Pathway A) or from a hydroxyl group (Pathway B) could take place. Pathway A leads to the formation of carbonyl groups by adding oxygenated functional groups to the carbon chain. In pathway B the resulting alkoxy radicals are decomposed via C-C bond scission, generating fragmentation products, as shown in Figure 9. The former case increases vapor pressure by approximately 1 order of magnitude, while the latter may increase volatility by a much larger degree by reducing the carbon number of the product molecules [42].

Irganox 1010 is a primary antioxidant, known as a H-donor and as radical scavenger. In accordance with the mechanism of oxidation of erythritol under air, two different alkyl radicals ( $R\bullet$ ) can be formed in pathway A, which in turn react with molecular oxygen to produce their corresponding peroxy radicals ( $ROO\bullet$ ). As mentioned before, oxidation of pathway B also produces alkoxy radicals ( $RO\bullet$ ). Primary antioxidants terminate oxidation by scavenging  $R\bullet$ ,  $ROO\bullet$  and  $RO\bullet$  radicals. In oxygen-rich conditions alkyl radicals react too fast with molecular oxygen and hence their lifetime is shortened enormously, which makes that alkyl radical scavenging become less important [46]. Irganox 1010 ( $ArOH$ ) converts peroxy and alkoxy radical into inactive products and phenoxy radicals ( $ArO\bullet$ ). Phenoxy radicals are less reactive; however, they still can react with other  $ROO\bullet/RO\bullet$  yielding non-radical products ( $ROO/ROArO$ ). These non-radical products can rearrange once to regenerate the phenolic antioxidant group, allowing further radicals to be scavenged [46,47]. However, once the antioxidant is fully consumed erythritol will begin to degrade as in the case of the long-term test under air.

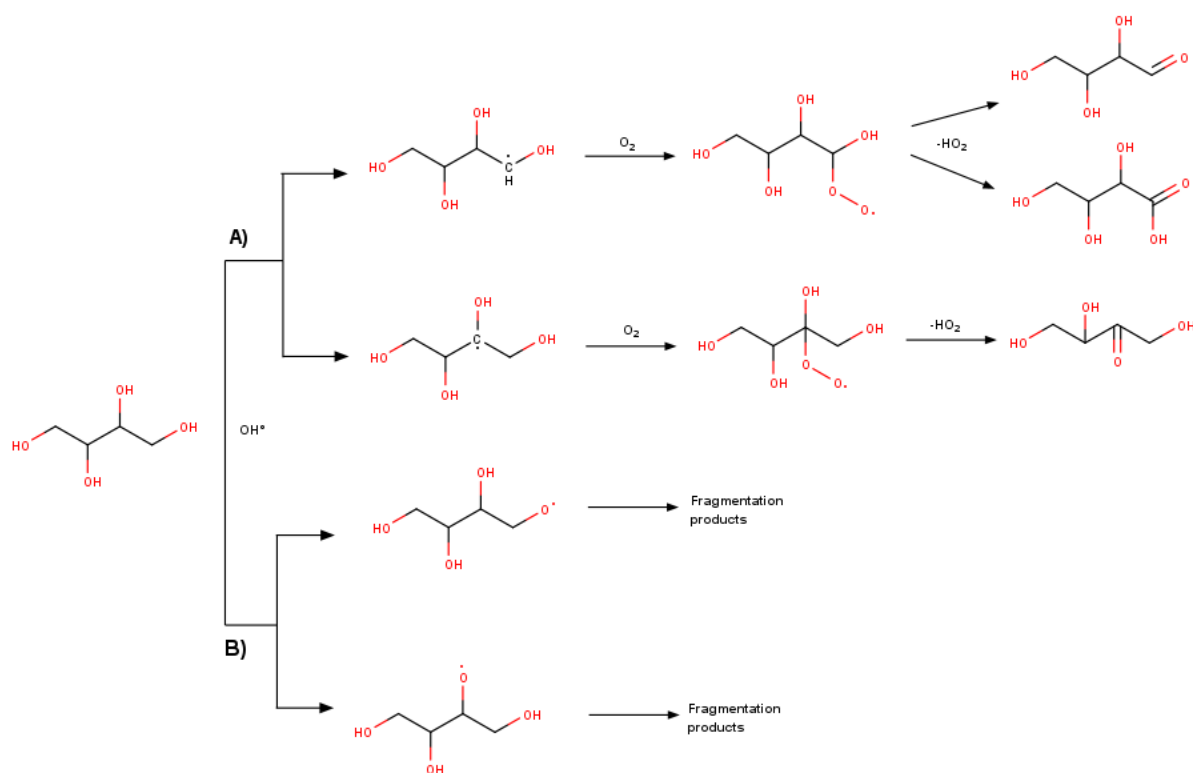


**Figure 9.** Proposed mechanism of oxidation of erythritol under air. Pathway A: abstraction of hydrogen atom to form alkyl radicals, which in the presence of oxygen are turned into peroxy radicals. Peroxy radicals can undergo the unimolecular HO<sub>2</sub> elimination process yielding carbonyl compounds. Pathway B: abstraction of hydrogen atoms to form alkoxy radicals, which undergo decomposition via C-C bond scission.

It has been reported that erythritol, as polyol, undergoes neither Maillard browning nor caramelization [48–50]. Even though some authors have suggested that the browning of sugar alcohols (D-mannitol) may be related to caramelization reactions [37,51], they have not detected sugar caramelization products, such as hydroxymethyl furfural (HMF) and hydroxyacetyl furan (HAF), but  $\alpha$ ,  $\beta$ -unsaturated carbonyl groups. However, these latter compounds may also be produced during dehydration reactions of polyols. Conjugated ketones, also known as enones, are a type of  $\alpha$ ,  $\beta$ -unsaturated carbonyl, which are found to be responsible for the color change in various systems. Conjugated ketones may have contributed to the brown coloration of a commercial pentaerythritol tetraester oil [52]. A slight yellowing of the polyvinyl chloride (PVC) was observed due to the formation of conjugated double bonds, which when increasing turned the PVC dark brown to finally black [53]. Color formation was also related to the increase of conjugated double bonds during thermal degradation of poly(L-lactic acid) (PLLA), as its UV-Vis spectra became stronger in intensity while the processing temperature increased [54]. Bayón and Rojas [37] also observed an increase of absorption in the UV-Vis spectra of D-mannitol when kept for longer times at 180 °C under air. In addition, they confirmed the occurrence of  $\alpha$ - $\beta$  unsaturated carbonyl groups, such as 4-methylpent-3-en-2-one, which display absorption bands between 240 nm and 320 nm, as a likely indicator of D-mannitol degradation. 4-methylpent-3-en-2-one is a well-known conjugated ketone generated in the aldol condensation of acetone on dehydration [55]. As mentioned before, erythritol became steadily brown with increasing temperature and time of thermal treatment, which is in good agreement with the time/temperature dependency of the formation of  $\alpha$ ,  $\beta$ -unsaturated carbonyl groups. In addition, Zeitsch [56] claimed that color build up in furfural is due to an increasing number of conjugated double bonds triggered by oxygen. Oxygen triggers discoloration by producing radicals, which attack the double bond of a furfural molecule leading to the formation of an uninterrupted sequence of conjugated double bonds. As already mentioned, pure

erythritol under air had the biggest color change after heating treatment, which suggests the formation of conjugated carbonyl systems from the oxidation products. Therefore, it is suggested that erythritol browning is rather related to the formation of conjugated carbonyl compounds when it oxidizes/dehydrates than to the caramelization process.

On the other hand, dehydration of erythritol at high temperatures has been reported [15,52,57]. The experimental method that Kakiuchi et al. [15] described is closer to the one used for this study, as erythritol under air was also heated up to 140 °C and kept there for a period of time. Even though the experimental conditions reported by the above-mentioned authors differ from each other, all of them confirmed 1,4-anhydroerythritol as the first reaction product of the dehydration of erythritol. Thus, not only oxygen concentration, but also temperature and heating time affect the dehydration process of erythritol. Bayón and Rojas [37] mentioned the formation, not only of cyclic ethers, but also of other products through different reaction pathways of thermal dehydration of polyols, giving place to the  $\alpha$ ,  $\beta$ -unsaturated carbonyl (or enones) groups. Intramolecular dehydration of polyols leads to cyclic ether production via an  $\text{SN}^2$  substitution process [58]. Intermolecular dehydration can lead to, among others, carbonyl compounds via a carbocation intermediate ( $\text{SN}^1$  mechanism) [59,60]. Ott [61] found the occurrence of carbonyl compounds via enolic intermediate by dehydration at the C-2 position of erythritol. Due to the occurrence of carbonyl compounds, many further possible subsequent reactions can follow, such as aldol additions and condensations, which in turn can give place to the  $\alpha$ ,  $\beta$ -unsaturated carbonyl groups mentioned also by Bayón and Rojas [37].

Figure 10a shows the FT-IR spectra of samples of pure erythritol under air before and after being heated. As temperature was raised, intermolecular hydrogen bonds weakened, and hence, the hydroxyl bonds strengthened [32]. This caused the  $\text{-OH}$  absorption band of unheated sugar alcohol ( $\sim 3225 \text{ cm}^{-1}$ ) to move to higher wave numbers (up to  $3240 \text{ cm}^{-1}$ ) at higher temperatures. The new peak that appeared at  $\sim 1716 \text{ cm}^{-1}$  in the thermally treated samples indicates the likely presence of carbonyl groups. In addition, a  $\text{C=O}$  stretching of a conjugated double bond of a ketone appeared at around  $1640 \text{ cm}^{-1}$  only for the heated samples [62]. This confirms the formation of conjugated carbonyl groups after heating treatment under air. As proposed, erythritol undergoes oxidation/dehydration reactions when heated under air. Both reactions give rise to carbonyl compounds and conjugated double bonds with similar absorptions bands. Hence, it is hard to confirm which one of the processes was the one that generated the products shown in the FTIR spectra.

Irganox 1010<sup>®</sup> contains ester linkages [63], which are represented by the absorption peak at  $\sim 1730 \text{ cm}^{-1}$  of the unheated samples in Figure 10. Heated samples with antioxidant under air (Figure 10c) show weak peak intensities at  $\sim 1730 \text{ cm}^{-1}$ . This is most likely due to the consumption of antioxidant during thermal treatment, since there was high oxygen availability. In contrast, Figure 10d shows stronger peak intensities at  $\sim 1730 \text{ cm}^{-1}$  for all heated samples. This could be related to a higher amount of antioxidant remaining in samples, as these were under argon atmosphere, and therefore, there was less oxygen to scavenge.

Unlike samples of pure erythritol under air, the FT-IR spectrum recorded for samples under argon atmosphere (Figure 10b) did not show significant changes either in the shape or in the wave numbers of absorption bands of carbonyl functional groups.

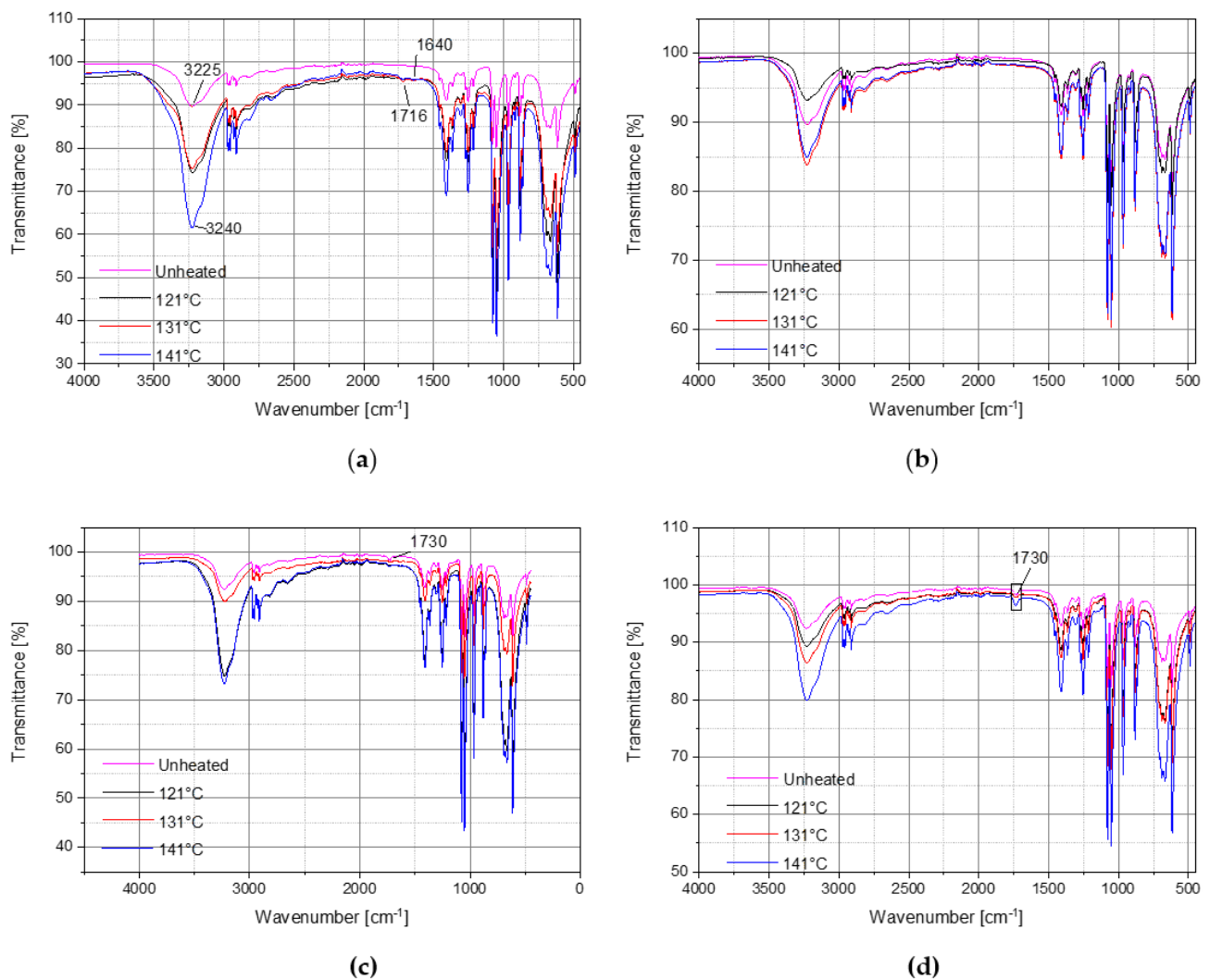


**Figure 10.** FT-IR spectra of the short-term-tests for (a) pure erythritol under air; (b) pure erythritol under argon atmosphere; (c) erythritol with antioxidant under air and (d) erythritol with antioxidant under argon atmosphere.

Lastly, Figure 11a depicts that after around 935 h of thermal treatment, in the long-term tests, two peaks appeared at  $\sim 1643\text{ cm}^{-1}$  and  $\sim 1725\text{ cm}^{-1}$  in samples of erythritol with antioxidant under air. As previously mentioned, absorption in this region corresponds to carbonyl groups. The C=O stretching of the conjugated ester is no longer visible ( $\sim 1730\text{ cm}^{-1}$ ), since the absorption bands corresponding to the oxidation/caramelization products overlap. However, it is likely that the antioxidant has been depleted during the long-term test, since as shown in Figure 10c, heated samples with antioxidant did not show absorption in the carbonyl groups region, while Figure 11a shows similar absorption bands as Figure 10a, which indicates an oxidation/dehydration process. Heated samples with antioxidant under air show only weaker peaks in the Irganox 1010<sup>®</sup> absorption region after 100 h of thermal treatment compared to their corresponding unheated sample (Figure 10c). In addition, as mentioned in Section 3.2, during the long-term test and only after 260 h, the degradation rate started to increase, which could be another hint about the antioxidant depletion. On the contrary, Figure 11b shows no chemical changes in pure erythritol under argon atmosphere after the long-term thermal treatment.

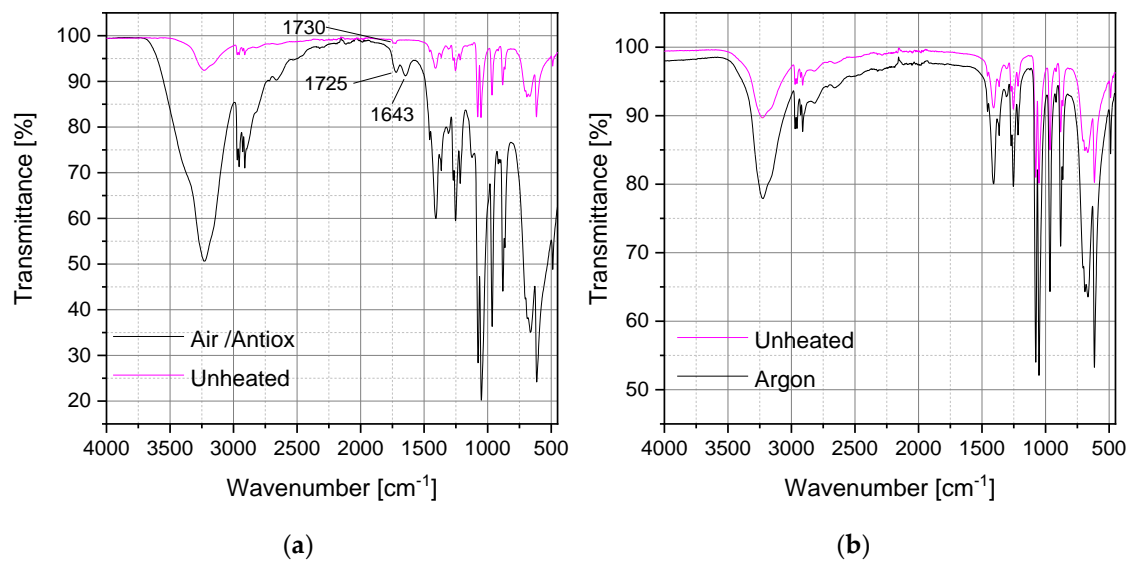


**Figure 11.** FT-IR spectra of the long-term-tests for (a) erythritol with antioxidant under air; (b) pure erythritol under argon atmosphere.

#### 4. Conclusions

Sugar alcohols belong to a promising category of organic phase change materials. Erythritol is an attractive sugar alcohol due to its thermal energy storage properties. However, earlier studies indicate that erythritol tends to degrade under thermal cycling. Most of the available studies report the structural changes of erythritol during cycling rather than its thermal stability at constant temperature, which would allow a degradation rate to be determined under conditions closer to real operation. In this study, the effect of thermal treatment above the melting point on the erythritol thermal, chemical and physical properties, as well as its degradation kinetics and the likely thermal stability enhancement by adding antioxidant and using it under inert atmosphere, were addressed.

The latent heat of erythritol under air decreased with the increasing temperature of thermal treatment as its hydrogen bonding structure was likely disrupted at high temperatures. In addition, a decrease in latent heat may also be attributed to incomplete crystallization during cooling from the melt.

Erythritol under air changed its color and some samples remained liquid after thermal treatment. Sample browning upon heating could be related to the formation of conjugated carbonyl compounds during oxidation/dehydration processes. Pure erythritol under air underwent glass transition as no exothermic peak was observed in its DSC thermogram during cooling. Erythritol under argon atmosphere, on the other hand, did solidify and its color barely changed.

Fragmentation products generated during oxidation and carbonyl compounds, among others, generated during dehydration increased the mass loss ratio in samples of pure erythritol under air. Antioxidant helped to reduce this effect.

FT-IR spectra of erythritol under air showed the occurrence of carbonyl groups and conjugated carbonyl compounds after thermal treatment. FT-IR spectra of erythritol under argon did not show new absorption bands, which confirmed its chemical stability after being heated above its melting temperature and up to 141 °C.

Minimal physical changes regarding color and consistency were observed in pure erythritol under argon atmosphere after being thermally treated, thus physical stability could be confirmed for up to 935 h of treatment. Finally, the degradation rate of latent heat was reduced from 0.19 kJ/(kg h) to 0.011 kJ/(kg h) when using an inert atmosphere.

**Author Contributions:** Conceptualization, M.P.A.L.; methodology, M.P.A.L.; investigation, M.P.A.L.; resources, M.P.A.L.; data curation, M.P.A.L.; writing—original draft preparation, M.P.A.L.; writing—review and editing, H.N. and S.G.; visualization, M.P.A.L.; supervision, H.N.; project administra-

tion, S.G.; funding acquisition, S.G. All authors have read and agreed to the published version of the manuscript.

**Funding:** This research was funded by the German Federal Ministry of Economics and Energy via several research projects, grant number 0325549A.

**Institutional Review Board Statement:** Not applicable.

**Informed Consent Statement:** Not applicable.

**Data Availability Statement:** The data presented in this study are available on request from the corresponding author. The data are not publicly available due to restrictions given by partners.

**Acknowledgments:** The authors are grateful to the Project Management Jülich for the administrative support.

**Conflicts of Interest:** The authors declare no conflict of interest.

## References

- Gude, V.G.; Nirmalakhandan, N.; Deng, S.; Maganti, A. Low temperature desalination using solar collectors augmented by thermal energy storage. *Appl. Energy* **2012**, *91*, 466–474. [CrossRef]
- Tian, Y.; Zhao, C. A review of solar collectors and thermal energy storage in solar thermal applications. *Appl. Energy* **2013**, *104*, 538–553. [CrossRef]
- N'Tsoukpoe, K.E.; Liu, H.; Le Pierrès, N.; Luo, L. A review on long-term sorption solar energy storage. *Renew. Sustain. Energy Rev.* **2009**, *13*, 2385–2396. [CrossRef]
- IEA IRENA. Thermal Energy Storage: Technology Brief E17. 2013. Available online: <https://www.irena.org/DocumentDownloads/Publications/IRENA-ETSAP20Tech20Brief20E1720Thermal20Energy20Storage.pdf> (accessed on 14 September 2018).
- Garg, H.; Mullick, S.C.; Bhargava, A.K. Sensible heat storage. In *Solar Thermal Energy Storage*; Garg, H.P., Mullick, S.C., Bhargava, A.K., Eds.; Springer: Dordrecht, The Netherlands, 1985; pp. 82–153.
- Mehling, H.; Cabeza, L.F. *Heat and Cold Storage with PCM: An Up to Date Introduction into Basics and Applications*; Springer: Berlin/Heidelberg, Germany, 2008.
- Kuznik, F.; David, D.; Johannes, K.; Roux, J.-J. A review on phase change materials integrated in building walls. *Renew. Sustain. Energy Rev.* **2011**, *15*, 379–391. [CrossRef]
- Ismail, K.; Henríquez, J.R. Thermally effective windows with moving phase change material curtains. *Appl. Therm. Eng.* **2001**, *21*, 1909–1923. [CrossRef]
- Weinläder, H.; Beck, A.; Fricke, J. PCM-facade-panel for daylighting and room heating. *Sol. Energy* **2005**, *78*, 177–186. [CrossRef]
- Boussaba, L.; Foufa, A.; Makhlof, S.; Lefebvre, G.; Royon, L. Elaboration and properties of a composite bio-based PCM for an application in building envelopes. *Constr. Build. Mater.* **2018**, *185*, 156–165. [CrossRef]
- del Barrio, E.P.; Godin, A.; Duquesne, M.; Daranlot, J.; Jolly, J.; Alshaer, W.; Kouadio, T.; Sommier, A. Characterization of different sugar alcohols as phase change materials for thermal energy storage applications. *Sol. Energy Mater. Sol. Cells* **2017**, *159*, 560–569. [CrossRef]
- Zhang, H.; Duquesne, M.; Godin, A.; Niedermaier, S.; Del Barrio, E.P.; Nedea, S.V.; Rindt, C.C. Experimental and in silico characterization of xylitol as seasonal heat storage material. *Fluid Phase Equilib.* **2017**, *436*, 55–68. [CrossRef]
- Gunasekara, S.N.; Pan, R.; Chiu, J.N.; Martin, V. Polyols as phase change materials for surplus thermal energy storage. *Appl. Energy* **2016**, *162*, 1439–1452. [CrossRef]
- Kaizawa, A.; Maruoka, N.; Kawai, A.; Kamano, H.; Jozuka, T.; Senda, T.; Akiyama, T. Thermophysical and heat transfer properties of phase change material candidate for waste heat transportation system. *Heat Mass Transf.* **2008**, *44*, 763–769. [CrossRef]
- Kakiuchi, H.; Yamazaki, M.; Yabe, M.; Chihara, S.; Terunuma, Y.; Sakata, Y.; Usami, T. A study of erythritol as phase change material. In Proceedings of the 2nd Workshop IEA Annex 10, Phase Change Materials and Chemical Reactions for Thermal Energy Storage, Sofia, Bulgaria, 11–13 April 1998.
- Nomura, T.; Tsubota, M.; Oya, T.; Okinaka, N.; Akiyama, T. Heat release performance of direct-contact heat exchanger with erythritol as phase change material. *Appl. Therm. Eng.* **2013**, *61*, 28–35. [CrossRef]
- Zhang, H.; van Wissen, R.M.J.; Nedea, S.V.; Rindt, C.C.M. Characterization of sugar alcohols as seasonal heat storage media—experimental and theoretical investigations. In Proceedings of the Advances in Thermal Energy Storage, EURO THERM 99, Lleida, Spain, 28–30 May 2014.
- Jesus, A.J.L.; Nunes, S.C.; Silva, M.R.; Beja, A.M.; Redinha, J. Erythritol: Crystal growth from the melt. *Int. J. Pharm.* **2010**, *388*, 129–135. [CrossRef] [PubMed]
- Diarce, G.; Gandarias, I.; Campos-Celador, Á.; García-Romero, A.; Griesser, U. Eutectic mixtures of sugar alcohols for thermal energy storage in the 50–90 °C temperature range. *Sol. Energy Mater. Sol. Cells* **2015**, *134*, 215–226. [CrossRef]
- Guo, S.; Liu, Q.; Zhao, J.; Jin, G.; Wang, X.; Lang, Z.; He, W.; Gong, Z. Evaluation and comparison of erythritol-based composites with addition of expanded graphite and carbon nanotubes. *Appl. Energy* **2017**, *205*, 703–709. [CrossRef]

21. Agyenim, F.; Eames, P.; Smyth, M. Experimental study on the melting and solidification behaviour of a medium temperature phase change storage material (Erythritol) system augmented with fins to power a LiBr/H<sub>2</sub>O absorption cooling system. *Renew. Energy* **2011**, *36*, 108–117. [CrossRef]
22. Kaizawa, A.; Kamano, H.; Kawai, A.; Jozuka, T.; Senda, T.; Maruoka, N.; Akiyama, T. Thermal and flow behaviors in heat transportation container using phase change material. *Energy Convers. Manag.* **2008**, *49*, 698–706. [CrossRef]
23. BASF. Industrial Coatings: Technical Data Sheet. Irganox 1010. 2015. Available online: [https://worldaccount.basf.com/wa/NAFTA~{jen\\_US/Catalog/Additives/info/BASF/PRD/30546637](https://worldaccount.basf.com/wa/NAFTA~{jen_US/Catalog/Additives/info/BASF/PRD/30546637) (accessed on 18 March 2019).
24. Zaharescu, T.; Giurginca, M.; Jipa, S. Radiochemical oxidation of ethylene–propylene elastomers in the presence of some phenolic antioxidants. *Polym. Degrad. Stab.* **1999**, *63*, 245–251. [CrossRef]
25. Gensler, R.; Plummer, C.; Kausch, H.-H.; Krämer, E.; Pauquet, J.-R.; Zweifel, H. Thermo-oxidative degradation of isotactic polypropylene at high temperatures: Phenolic antioxidants versus HAS. *Polym. Degrad. Stab.* **2000**, *67*, 195–208. [CrossRef]
26. Sagara, A.; Nomura, T.; Tsubota, M.; Okinaka, N.; Akiyama, T. Improvement in thermal endurance of D-mannitol as phase-change material by impregnation into nanosized pores. *Mater. Chem. Phys.* **2014**, *146*, 253–260. [CrossRef]
27. Vyazovkin, S.; Sbirrazzuoli, N. Kinetic methods to study isothermal and nonisothermal epoxy-anhydride cure. *Macromol. Chem. Phys.* **1999**, *200*, 2294–2303. [CrossRef]
28. Vyazovkin, S.; Wight, C.A. Model-free and model-fitting approaches to kinetic analysis of isothermal and nonisothermal data. *Thermochim. Acta* **1999**, *340*, 53–68. [CrossRef]
29. Halikia, I.; Zoumpoulakis, L.; Christodoulou, E.; Prattis, D. Kinetic study of the thermal decomposition of calcium. *Eur. J. Miner. Process. Environ. Prot.* **2001**, *1*, 89–102.
30. Neumann, H.; Niedermaier, S.; Gschwander, S.; Schossig, P. Cycling stability of d-mannitol when used as phase change material for thermal storage applications. *Thermochim. Acta* **2018**, *660*, 134–143. [CrossRef]
31. Solé, A.; Neumann, H.; Niedermaier, S.; Martorell, I.; Schossig, P.; Cabeza, L.F. Stability of sugar alcohols as PCM for thermal energy storage. *Sol. Energy Mater. Sol. Cells* **2014**, *126*, 125–134. [CrossRef]
32. Feng, H.; Liu, X.; He, S.; Wu, K.; Zhang, J. Studies on solid-solid phase transitions of polyols by infrared spectroscopy. *Thermochim. Acta* **2000**, *348*, 175–179. [CrossRef]
33. Wu, N.; Li, X.; Liu, S.; Zhang, M.; Ouyang, S. Effect of hydrogen bonding on the surface tension properties of binary mixture (acetone-water) by Raman spectroscopy. *Appl. Sci.* **2019**, *9*, 1235. [CrossRef]
34. Inagaki, T.; Ishida, T. Computational design of non-natural sugar alcohols to increase thermal storage density: Beyond existing organic phase change materials. *J. Am. Chem. Soc.* **2016**, *138*, 11810–11819. [CrossRef]
35. Matuszek, K.; Vijayaraghavan, R.; Kar, M.; Macfarlane, D.R. Role of hydrogen bonding in phase change materials. *Cryst. Growth Des.* **2019**, *20*, 1285–1291. [CrossRef]
36. Nomura, T.; Zhu, C.; Sagara, A.; Okinaka, N.; Akiyama, T. Estimation of thermal endurance of multicomponent sugar alcohols as phase change materials. *Appl. Therm. Eng.* **2015**, *75*, 481–486. [CrossRef]
37. Bayón, R.; Rojas, E. Feasibility study of D-mannitol as phase change material for thermal storage. *AIMS Energy* **2017**, *5*, 404–424. [CrossRef]
38. Nakano, K.; Masuda, Y.; Daiguji, H. Crystallization and melting behavior of erythritol in and around two-dimensional hexagonal mesoporous silica. *J. Phys. Chem. C* **2015**, *119*, 4769–4777. [CrossRef]
39. Dougherty, R.C. Temperature and pressure dependence of hydrogen bond strength: A perturbation molecular orbital approach. *J. Chem. Phys.* **1998**, *109*, 7372–7378. [CrossRef]
40. Burgoa, A.; Hernandez, R.; Vilas, J.L. New ways to improve the damping properties in high-performance thermoplastic vulcanizates. *Polym. Int.* **2020**, *69*, 467–475. [CrossRef]
41. Zhang, L.; Chen, D.; Fan, X.; Cai, Z.; Zhu, M. Effect of hindered phenol crystallization on properties of organic hybrid damping materials. *Materials* **2019**, *12*, 1008. [CrossRef] [PubMed]
42. Kessler, S.H.; Smith, J.D.; Che, D.L.; Worsnop, D.R.; Wilson, K.R.; Kroll, J.H. Chemical sinks of organic aerosol: Kinetics and products of the heterogeneous oxidation of erythritol and levoglucosan. *Environ. Sci. Technol.* **2010**, *44*, 7005–7010. [CrossRef] [PubMed]
43. George, I.J.; Abbatt, J.P.D. Heterogeneous oxidation of atmospheric aerosol particles by gas-phase radicals. *Nat. Chem.* **2010**, *2*, 713–722. [CrossRef] [PubMed]
44. Kroll, J.H.; Lim, C.; Kessler, S.H.; Wilson, K.R. Heterogeneous oxidation of atmospheric organic aerosol: Kinetics of changes to the amount and oxidation state of particle-phase organic carbon. *J. Phys. Chem. A* **2015**, *119*, 10767–10783. [CrossRef]
45. den Hartog, G.J.; Boots, A.W.; Adam-Perrot, A.; Brouns, F.; Verkooijen, I.W.; Weseler, A.R.; Haenen, G.R.; Bast, A. Erythritol is a sweet antioxidant. *Nutrients* **2010**, *26*, 449–458. [CrossRef] [PubMed]
46. Gijssman, P. Polymer stabilization. In *Handbook of Environmental Degradation of Materials*, 3rd ed.; Kutz, M., Ed.; William Andrew: Oxford, UK, 2018; pp. 369–395.
47. Frankel, E.N. (Ed.) Chapter 9—Antioxidants. In *Lipid Oxidation*, 2nd ed.; Oily Press Lipid Library Series; Woodhead Publishing: Cambridge, UK, 2012; pp. 209–258.
48. Ghosh, S.; Sudha, M.L. A review on polyols: New frontiers for health-based bakery products. *Int. J. Food Sci. Nutr.* **2011**, *63*, 372–379. [CrossRef]

49. Grembecka, M. Sugar alcohols as sugar substitutes in food industry. In *Sweeteners: Pharmacology, Biotechnology, and Applications*; Mérillon, J.-M., Ramawat, K.G., Eds.; Springer International Publishing: Cham, Switzerland, 2018; pp. 547–573.
50. Hartel, R.W.; von Elbe, J.H.; Hofberger, R. Chemistry of bulk sweeteners. In *Confectionery Science and Technology*; Springer Science and Business Media LLC: Berlin, Germany, 2017; pp. 3–37.
51. Rodríguez-García, M.-M.; Bayón, R.; Rojas, E. Stability of D-mannitol upon melting/freezing cycles under controlled inert atmosphere. *Energy Procedia* **2016**, *91*, 218–225. [[CrossRef](#)]
52. Karis, T.E.; Miller, J.L.; Hunziker, H.E.; de Vries, M.S.; Hopper, D.A.; Nagaraj, H.S. Oxidation chemistry of a pentaerythritol tetraester oil. *Tribol. Trans.* **1999**, *42*, 431–442. [[CrossRef](#)]
53. Schiller, M. PVC Stabilizers. In *PVC Additives: Performance, Chemistry, Developments and Sustainability*; Hanser: Munich, Germany, 2015; pp. 1–114.
54. Wang, Y.; Steinhoff, B.; Brinkmann, C.; Alig, I. In-line monitoring of the thermal degradation of poly(l-lactic acid) during melt extrusion by UV-vis spectroscopy. *Polymer* **2008**, *49*, 1257–1265. [[CrossRef](#)]
55. Pauwels, D.; Hereijgers, J.; Verhulst, K.; de Wael, K.; Breugelmans, T. Investigation of the electrosynthetic pathway of the aldol condensation of acetone. *Chem. Eng. J.* **2016**, *289*, 554–561. [[CrossRef](#)]
56. Zeitsch, K.J. (Ed.) The discoloration of furfural. In *The Chemistry and Technology of Furfural and Its Many By-Products*; Elsevier: Amsterdam, The Netherlands, 2000; pp. 28–33.
57. Ott, L.; Lehr, V.; Urfels, S.; Bicker, M.; Vogel, H. Influence of salts on the dehydration of several biomass-derived polyols in sub- and supercritical water. *J. Supercrit. Fluids* **2006**, *38*, 80–93. [[CrossRef](#)]
58. Yamaguchi, A.; Muramatsu, N.; Mimura, N.; Shirai, M.; Sato, O. Intramolecular dehydration of biomass-derived sugar alcohols in high-temperature water. *Phys. Chem. Chem. Phys.* **2016**, *19*, 2714–2722. [[CrossRef](#)]
59. Vilcocq, L.; Cabiac, A.; Especel, C.; Guillon, E.; Duprez, D. Transformation of sorbitol to biofuels by heterogeneous catalysis: Chemical and industrial considerations. *Oil Gas Sci. Technol. Rev. IFP Energ. Nouv.* **2013**, *68*, 841–860. [[CrossRef](#)]
60. Kurszewska, M.; Skorupa, E.; Kasprzykowska, R.; Sowiński, P.; Wiśniewski, A. The solvent-free thermal dehydration of tetritols on zeolites. *Carbohydr. Res.* **2000**, *326*, 241–249. [[CrossRef](#)]
61. Ott, L. Stoffliche Nutzung von Biomasse mit Hilfe von nah- und überkritischen Wasser: Homogenkatalysierte Dehydratisierung von Polyolen zu Aldehyden. Ph.D. Thesis, Technische Universität Darmstadt, Darmstadt, Germany, 2005.
62. Coates, J. Interpretation of infrared spectra, a practical approach. In *Encyclopedia of Analytical Chemistry: Applications, Theory and Instrumentation*; Meyers, R.A., Ed.; John Wiley & Sons Ltd.: Chichester, UK, 2000.
63. Ratnam, C.T.; Nasir, M.; Baharin, A.; Zaman, K. Electron-beam irradiation of poly(vinyl chloride)/epoxidized natural rubber blend in the presence of Irganox 1010. *Polym. Degrad. Stab.* **2001**, *72*, 147–155. [[CrossRef](#)]